Thermodynamic and Structural Investigation of Thermoreversible Poly(3-dodecyl thiophene) Gels in the Three Isomers of Xylene

Sudip Malik and Arun K. Nandi*

Polymer Science Unit, Indian Association for the Cultivation of Science, Jadavpur, Kolkata 700 032, India

Received: September 1, 2003; In Final Form: October 28, 2003

Poly(3-dodecyl thiophene) (P3DDT) produces thermoreversible gels in *o*-, *m*-, and *p*-xylene (Xy). All of these gels have fibrillar network morphology and exhibit reversible first-order phase transitions. The enthalpy changes related to the polymer part of P3DDT−*p*-Xy gels indicate polymer−solvent complex formation having stoichiometry of P3DDT monomeric unit/*p*-Xy = 2:3. In P3DDT−*o*-Xy and P3DDT−*m*-Xy gels, the enthalpy changes also indicate similar polymer−solvent complexation of 2:3 type. In our experimental condition, only *p*-Xy crystallizes, and analysis of its enthalpy changes indicate the formation of a polymer−solvent complex of stoichiometry P3DDT monomeric unit/*p*-Xy = 3:1. In the phase diagrams, there are main chain melting and side chain melting boundaries; the latter encompasses the whole composition region. In the P3DDT−*p*-Xy system, there is an additional solvent melting boundary. The phase diagram nature suggests that the 2:3 complex is singular type. The solvent-subtracted Fourier-transform infrared (FTIR) spectra showed different absorbance peaks in the gels of different compositions and are attributed to the different polymer−solvent complexes produced in the gels. Wide-angle x-ray scattering (WAXS) study indicated an increase in the lamellar thickness with decreasing P3DDT concentration in the gel, and the intensity ratio of the diffraction peaks also changes from those of the polymer melt. The lamella structure is absent in the dilute gel (W_{P3DDT} = 0.14) indicating that dilute gels have different structure than concentrated gels (W_{P3DDT} = 0.59 and 0.86) have. Molecular modeling using MMX program supports the increase of interchain lamellar thickness of P3DDT chain with incorporation of *p*-Xy molecules.

Introduction

Poly(3-alkyl thiophenes) (P3ATs) are important electroactive polymers because of their wide range of applicability in nonlinear optical devices, electroactive devices, light emitting diodes, etc.[1] These properties and conductivity of P3ATs depend on the preparation procedure, for example, the spin-coated films have conductivity two orders higher than that of the solvent-cast samples.[2] Also films slowly dried from gels have one order increase in conductivity over that of the cast films.[3] In our earlier work, we reported that poly(3-hexyl thiophene) (P3HT) produces a thermoreversible gel in xylene, and this is also true for regioregular poly(3-octyl thiophene) (P3OT) and poly(3-dodecyl thiophene) (P3DDT).[4] It is now established that solvent has a strong influence on the gelation process, for example, syndiotactic polystyrene shows fibrillar network[5] in benzene and toluene but not in *trans*-decalin, so to understand the gelation processes more completely, the thermodynamic study is very important.[6−12] It may enable one to know about the polymer−solvent complexation from the enthalpy change during gelation, the phase diagrams of the gels, and finally the macroscopic cause of gelation. P3ATs are comblike polymers and have interchain lamellar structure in the solid state.[13,14] The interchain lamella are produced mainly from the side chain crystallization of the P3AT chains. A gel-forming solvent may affect both the side chain and main chain crystallization; consequently, new thermodynamic properties may develop in these gels. Xylene has three isomers, for example, ortho, meta, and para isomers, and they may behave differently in the gelation process.[5]

There are some reports on the thermodynamic study of thermoreversible gels in the literature.[6−12,15−20] To make a generalization of thermodynamic behavior of these gels is difficult, as it depends on the individual polymer−solvent system. Recently, Liu and Pandey[18] attempted to make a generalization of thermodynamics of sol−gel transition using a Monte Carlo simulation model. The thermodynamic study of the P3AT gels is not yet reported in the literature. P3ATs during gelation undergo coil-to-rod transformation in poor solvents.[3,4,21] The phase behavior of rodlike polymer is very complex as both isotropic and liquid crystalline phases coexist over some concentration range.[22,23] Again the side chains of P3ATs are capable of crystallization[13,14,24,25] along with the formation of main chain crystals. All of these phases, for example, side chain crystals, main chain crystals, and liquid crystalline phases, are capable of gelation.[26] Besides, during gelation polymer−solvent complexation may also take place.[6−8,10−11,17−18] So the thermodynamic study of these gels is necessary to understand precisely the macroscopic cause of gelation for this important polymer. In this manuscript, the thermal behavior of the gels, the enthalpy changes, the phase diagrams, etc. are worked out. P3DDT and *ortho*-, *meta*-, and *para*-xylene are used in this work. P3DDT is chosen for its lower melting point than those of the other members (e.g., hexyl and octyl), and therefore, it helps to minimize any solvent evaporation during the thermal investigation. The structure of P3DDT is shown in Scheme 1. The X-ray, Fourier-transform infrared (FTIR), and molecular modeling techniques were used to get an idea about the structure of the gels and hence to substantiate the thermal results.

* To whom correspondence should be addressed. E-mail: psuakn@mahendra.iacs.res.in.

10.1021/jp036590f CCC: $27.50
Published on Web 12/11/2003

SCHEME 1: Structure of Poly(3-dodecyl thiophene) Showing Head−Tail, Head−Head, and Tail−Tail Linkages

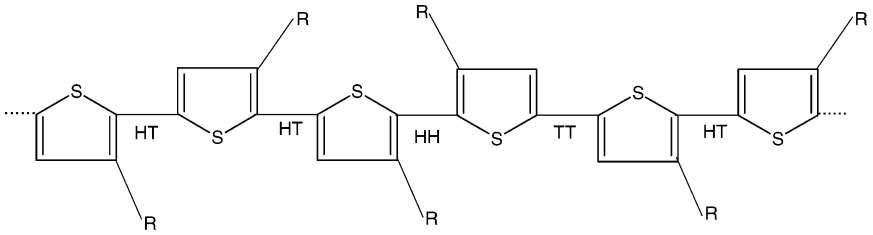

TABLE 1: Characteristics of Sample and Solvents

	molecular weight (M_w) $\times 10^{-4}$	H−T regioregularity (±2 mol %)	melting point (°C)	boiling point (°C)	density (g/ mL)
poly(3-dodecyl thiophene) (P3DDT)	16.2	88	180[a]		1.07
para-xylene (*p*-Xy)			18.4	189	0.866
ortho-xylene (*o*-Xy)			−25	144	0.870
meta-xylene (*m*-Xy)			−48	139	0.868

[a] Equilibrium melting point.[24]

Experimental Section

Samples. Regioregular P3DDT sample was purchased from Aldrich Chemicals Co., and as reported by the company, it was prepared by Rieke's method.[27] It was dissolved in $CHCl_3$ and was filtered off the suspended impurities present within it. The solutions were evaporated to dryness in a pool of air and were finally dried in a vacuum at 50 °C for 5 days. The head-to-tail regioregularity was measured from ^1H NMR spectroscopy in a Bruker 300 MHz instrument.[28] The solvents *o*-, *m*-, and *p*-xylene were also purchased from Aldrich Chemicals Co., and the characteristics of the sample and the solvents are presented in Table 1.

Preparation and Characterization of Gels. The gels were prepared in two different ways. For scanning electron microscopy (SEM), wide-angle x-ray scattering (WAXS) and FTIR investigations, the gels were prepared in sealed glass tubes, and for thermal study, they were prepared in Perkin-Elmer large volume capsules (LVC). In glass tubes, a weighed amount of polymer and solvent was sealed in a vacuum (10^{-3} mmHg) after degassing by repeated freeze−thaw technique. They were made homogeneous at 150 °C and were gelled by quenching the tube at 0 °C for 30 min. For SEM study, the gels were taken out of the tube and dried at room temperature (25 °C) in a pool of air and finally in a vacuum at 25 °C for 5 days. Care was taken that during the drying process the gel had not melted. They were then gold-coated, and their micrographs were recorded in a SEM apparatus (Hitachi S-2300). For WAXS study, the gels were put on a glass holder, and the X-ray diffractograms were obtained from a Seifert X-ray diffractometer (3000) with a parallel beam optics attachment. The instrument was operated at 35 kV voltage and 30 mA current and was calibrated with standard silicon sample. The samples were scanned at the step scan mode (step size 0.03°, preset time 1 s), and the diffraction pattern was recorded with the help of a scintillation counter detector. The FTIR studies of the gels were done in a Nicolet instrument [Magna IR-750 spectrometer (series-II)]. A small portion of the gel/solvent was taken between two KBr pellets and was scanned to average over 40 scans. In each experiment, the same amount of gel was placed in a similar fashion between the two KBR pellets. The solvent spectrum was then subtracted from the gel spectra using the software of the instrument to obtain the P3AT spectra in the gel form.

Thermal Study. In LVC capsules, a weighed amount of polymer (3−7 mg) and solvent in required amount were sealed with the help of a quick press. They were made homogeneous at temperatures 10 °C below the boiling temperature of the respective solvent for 10 min. They were then quenched at the rate of 40 °C/min to −30 °C where they were kept for 60 min. They were then heated at the rate of 10 °C/min in a DSC-7 (Perkin-Elmer), and the thermograms were recorded in a computer attached to the instrument. Also a cooling run from 180 °C at the rate of 5 °C/min was performed to obtain the gelation exotherms. The gel melting temperature, gelation temperature, and their corresponding enthalpies were measured from the thermograms with help of the computer. The instrument was calibrated with indium before each set of experiments.

Molecular Modeling. To get an approximate idea of molecular structure of P3AT gels, molecular modeling of the pure polymer and its gel was performed using a molecular mechanics (MMX) program.[29] For simplicity, two P3DDT chains each with 10 repeating units were chosen and were drawn to give a probable lamellar structure. They were then energetically minimized with the help of the MMX program in a computer. During the formation of molecular models of P3DDT−*p*-Xy complexes, *p*-Xy molecules in required proportions were incorporated into the vacant places at the end of dodecyl chains and were energetically minimized. The interchain lamellar distances and other distances were enquired using the program.

Results and Discussion

In Figure 1, a representative SEM picture of dried gel of $W_{P3DDT} = 0.10$ in *p*-xylene is presented. The gel consists of fibrillar network structures, and it is assumed throughout the work that the gel structure remains unchanged during the drying process. The *o*-xylene and *m*-xylene also yield similar fibrillar network structure. In Figure 2a,b, the representative differential scanning calorimetry (DSC) thermograms of P3DDT gels in *p*-xylene are presented for the gel melting process. In Figure 2a, there is a large melting peak at the temperature range 15−20 °C, and there are small melting peaks at higher temperature for all compositions. To visualize the latter peaks better, the enlarged thermograms of the high-temperature region are presented in Figure 2b. The peak corresponding to 75 °C is the side chain melting peak, while those at 110−140 °C are due to

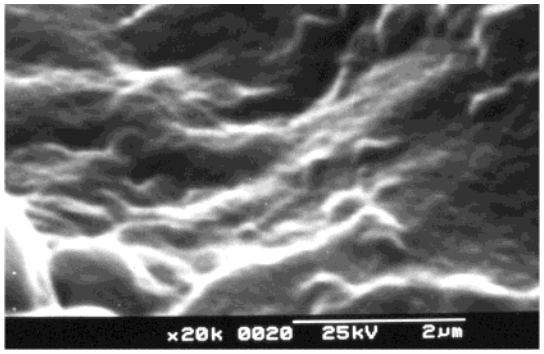

Figure 1. A representative SEM micrograph of dried gels of regioregular P3DDT in *p*-Xy ($W_{P3DDT} = 0.10$).

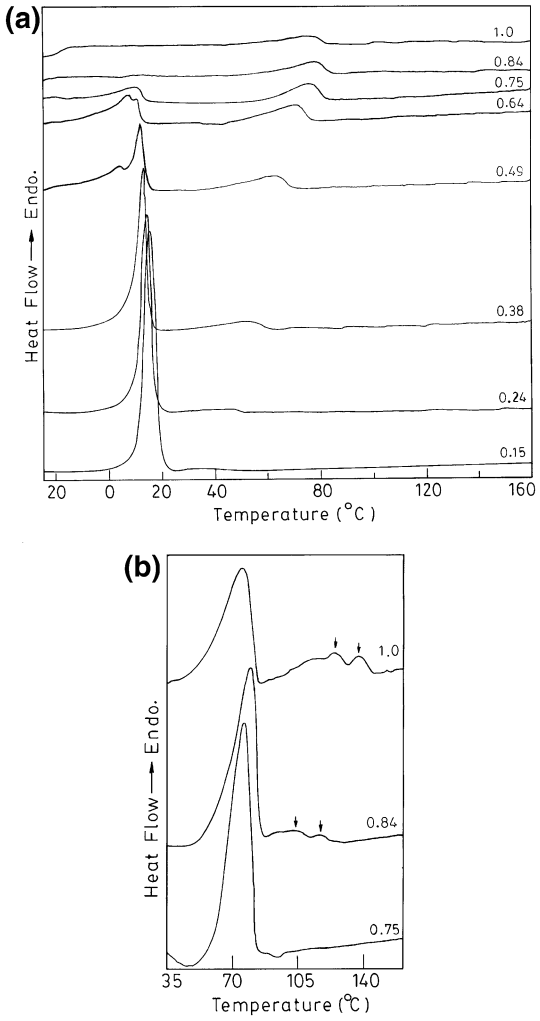

Figure 2. The representative melting thermograms (a) of P3DDT−*p*-Xy gels at indicated weight fractions of P3DDT and (b) enlarged portion of the polymer part of the thermogram.

the main chain melting peaks. The origin of the two main chain melting peaks in P3DDT is not completely understood. Park and Levon[13] proposed from their DSC and optical microscopic results that the low-temperature peak is due to the melting of P3DDT crystal and the higher one is related to isotropization of the less ordered phase developed by the restriction of crystallization due to the increase of sample viscosity. Liu and Chung,[25] however, argued that the lower one is the melting of the crystalline ordered phase and the highest one is due to the melting of the ordered phase produced from the zipping effect of the side chain. Without going to the controversy, we shall

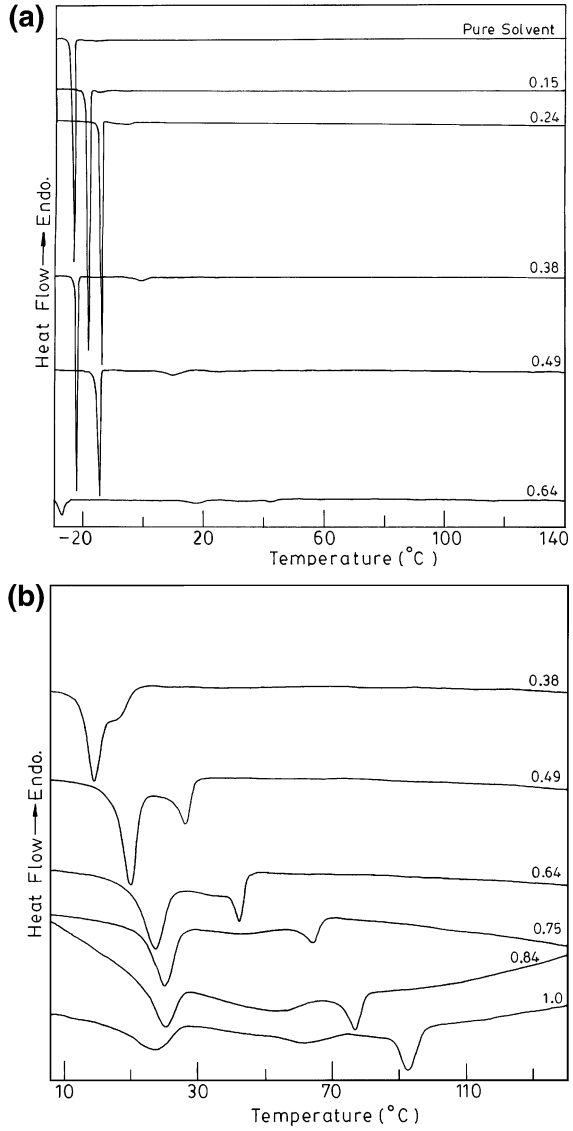

Figure 3. Cooling thermograms (a) of P3DDT−*p*-Xy gels for indicated compositions and (b) enlarged portion of the polymer part of the cooling thermograms.

consider both of the peaks as the melting peaks of the main chain crystals for two different states (PS_1 and PS_2). It is important to note that the main chain melting peaks are not observed for the gel composition $W_{P3DDT} \leq 0.75$ (W_{P3DDT} represents the weight fraction of P3DDT in the gel), while the side chain melting peak exists over the whole composition range. The exact cause for the disappearance of main chain melting peaks is not known. The probable reasons are as follows: (i) *p*-xylene dilutes the P3DDT main chain preventing its crystallization, (ii) polymer−solvent complex formation makes the main chain unable to crystallize, and (iii) the main chain melting peak overlaps with the side chain melting peak. The side chains being regular and flexible easily produce crystallites even in the diluted condition. Of particular interest is that the solvent melting peak bifurcates at the concentration range $W_{P3DDT} = 0.49-0.64$, and this probably indicates that the solvent in these gels may experience two different environments yielding two different melting points.

In Figure 3a,b, representative cooling thermograms of P3DDT−*p*-Xy gels of different compositions are presented. The enlarged cooling thermograms at higher temperature portion (Figure 3b) exhibit three exothermic peaks up to the composition W_{P3DDT}

= 0.54. In $W_{P3DDT} = 0.49-0.38$, they are doublet, and below that it is single. Thus a difference in behavior of the heating and cooling thermograms (Figure 2b and 3b) is observed. So it may be argued that the disappearance of main chain melting peaks for compositions $W_{P3DDT} \leq 0.75$ might be due to the overlapping with the side chain melting peak. The origin of the three exothermic peaks in the cooling thermograms (Figure 3b) is not certain, and it may be proposed that the two higher temperature peaks are due to main chain crystallization and the lower one is for the side chain crystallization. With gradual increase of solvent concentration, the middle peak gradually disappears, and with further dilution, the other main chain crystallization peak also vanishes. The side chain crystallization peak, however, remains throughout the whole composition range studied here indicating that side chain crystallization may be a cause for gelation. In P3DDT−*o*-Xy and P3DDT−*m*-Xy gels, melting endotherms are similar to P3DDT−*p*-Xy gels except for the absence of solvent melting peak at ∼15 °C. The cooling thermograms of these systems also exhibit three exothermic peaks for gels with higher W_{P3DDT}, and with dilution it becomes doublet, and on further dilution, it yields a single exothermic peak. The difference with that of P3DDT−*p*-Xy system is the absence of the solvent crystallization peak. In the following section, the enthalpy changes during both heating and cooling processes and the phase diagrams derived from the peak temperatures will be discussed.

Enthalpy Changes. *Polymer Part.* In Figure 4a−c, the variation of enthalpy changes (ΔH of the polymer part) with W_{P3DDT} are shown for both heating and cooling processes. The enthalpy changes are almost the same for both of the processes, and this supports our earlier contention that some of the main chain melting peaks overlapped with the side chain melting peaks. All of the ΔH data are above the straight line joining those of the pure components, indicating a positive deviation from linearity.[8,17−18] The enthalpy of gel melting may be considered to consist of three contributions:[8]

$$\Delta H^{(\text{pergm})} = w_1 \Delta H_1 + w_2 \Delta H_2 + \Delta H_c \qquad (1)$$

where w represents the weight fraction and subscripts 1 and 2 represent the xylene and the polymer, respectively. ΔH_i represents the melting enthalpy of each component, and ΔH_c is the enthalpy change for the melting of any polymer−solvent assembled (complex) structure formed during gelation. In the case of gel formation, the same notation follows where ΔH represents the enthalpy of formation in each case. For the P3DDT−*p*-Xy system, the melting and crystallization peaks of *p*-Xy are far apart from the melting/crystallization peaks of side chain and main chain crystals of polymer. In our calculation of ΔH (total enthalpy change for polymer peaks), the contribution of *p*-xylene was not considered. So for this system under this condition, ΔH_1 may be approximated as zero. Consequently,

$$\Delta H - w_2 \Delta H_2 = \Delta H_c \qquad (2)$$

In the cases of P3DDT−*o*-Xy and P3DDT−*m*-Xy systems, solvents do not crystallize under the experimental conditions. Consequently, eq 2 applies well to these systems. The left-hand side of eq 2 is the positive deviation (Δ) from linearity [Figure 4a−c]. The deviation Δ when plotted with W_{P3DDT} may yield a maximum, and the composition of the maximum corresponds to the composition of the polymer−solvent complex[6,8,10−11,17,30] formed in the gel. In the Δ versus W_{P3DDT} plots [Figure 5a−c], there are maxima at $W_{P3DDT} \approx 0.60$ for all of the systems. These results, therefore, indicate that polymer−solvent complexation occurs in all of the P3DDT−Xy gels with the molar composition of P3DDT monomer unit/xylene = 2:3.

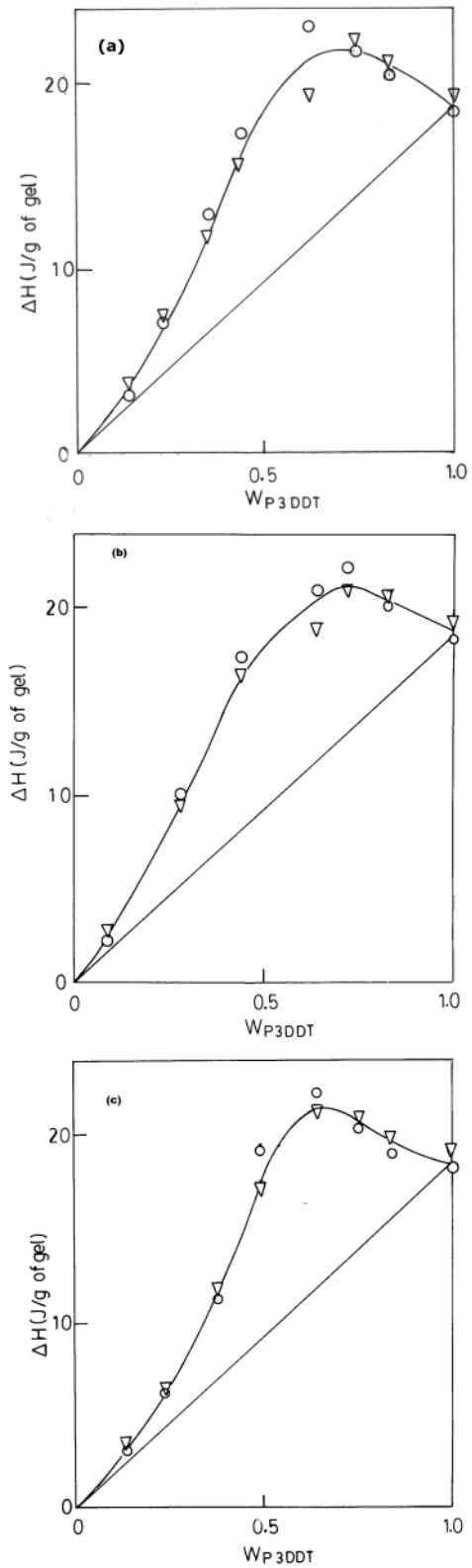

Figure 4. Plot of enthalpy changes of polymer part during the gel melting/gelation process of P3DDT−xylene gels vs W_{P3DDT}: (○) gel melting; (▽) gelation; (a) *p*-Xy; (b) *o*-Xy; (c) *m*-Xy.

Solvent Part. The *o*-xylene and *m*-xylene do not crystallize during our experimental condition, whereas *p*-xylene crystallizes at −28 °C. Here we analyze separately the *p*-xylene melting/crystallization peaks of the thermograms of Figures 2 and 3 to

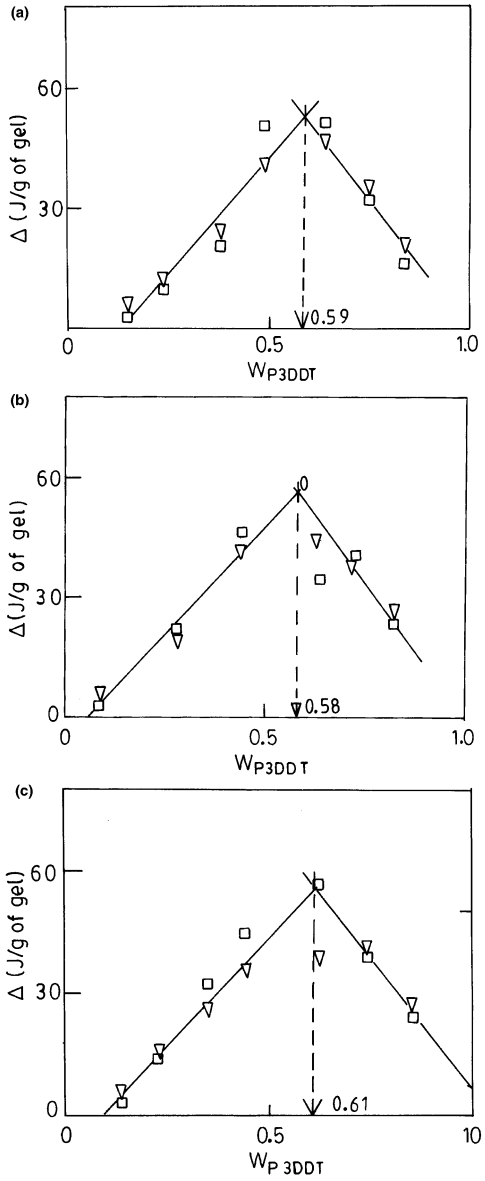

Figure 5. Plot for the deviation (Δ) vs W_{P3DDT} for the P3DDT gel in (a) *p*-Xy, (b) *o*-Xy, and (c) *m*-Xy. Arrows indicate the compositions of the complexes.

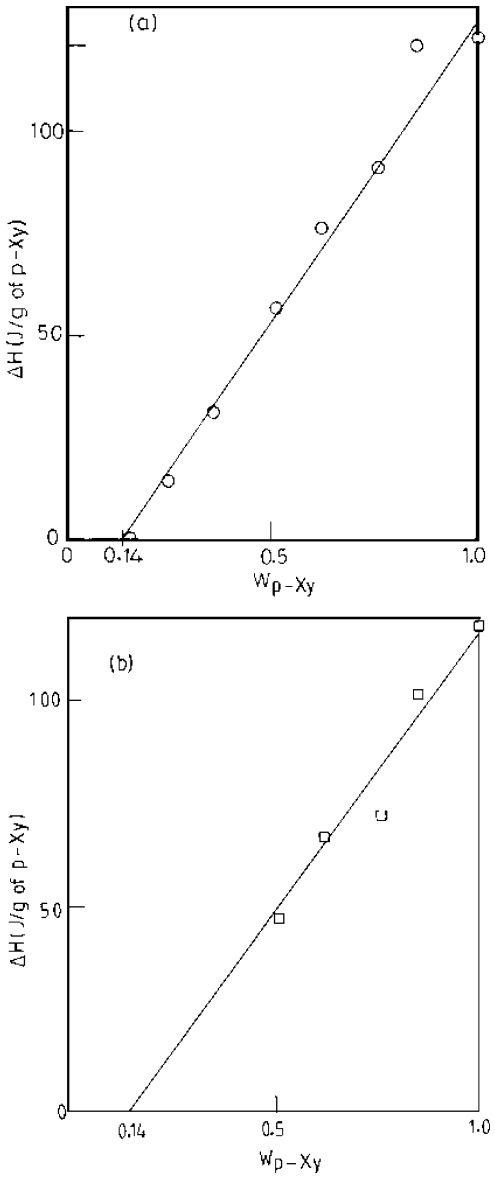

Figure 6. Enthalpy changes of the solvent (*p*-Xy) during the gel melting/gelation process of P3DDT−*p*-xylene gel vs W_{p-Xy} plot: (a) heating experiment; (b) cooling experiment.

get more idea of polymer−solvent complexation in the gels. In Figure 6a,b, Δ*H* values of both heating and cooling processes are plotted with W_{p-Xy}. It is apparent from the figure that with decreasing *p*-xylene concentration Δ*H* decreases, and it becomes zero at $W_{p-Xy} = 0.14$ for both of the processes. The absence of solvent peak at this composition may be due to the complete use of the solvent to form polymer−solvent complexes, and this composition ($W_{P3DDT} = 0.86$) corresponds to a polymer−solvent complex of stoichiometry P3DDT monomer unit/*p*-xylene = 3:1. Thus the analysis of enthalpy of fusion of the polymer part indicates the formation of a polymer−solvent complex of 2:3 type, whereas that of the solvent part indicates the formation of a polymer−solvent complex of 3:1 type. So two different polymer−solvent complexes are evidenced in this gel, and this is similar to *syn*-PMMA−bromobenzene, *syn*-PMMA−chlorobenzene, and *syn*-polystyrene−benzene gels.[10,30]

The Phase Diagram of Gels. The phase diagrams of P3DDT−*p*-Xy, P3DDT−*o*-Xy, and P3DDT−*m*-Xy gels are shown in Figure 7a−c. It is apparent from the figure that the side chain crystal melting encompasses the whole gel composition but the main chain melting encompasses up to a certain concentration of the polymer ($W_{P3DDT} \approx 0.75$). From the side chain melting, it is apparent that polymer−solvent complex (2:3) (C_1) is of singular type (intermediate between congruent and incongruent).[6,31] In these melting peaks, we could not observe any separate peak for the compound. So it may be surmised that each side chain endotherm is actually composed of two indistinguishable peaks.[8,17,18] The first of these indistinguishable peak corresponds to the transformation of

$$\underset{(2:3)}{\text{compound}} \rightarrow \underset{(3:1)}{\text{compound}} + \text{solvent} \qquad (3)$$

and is nonvariant with composition, whereas the second peak corresponds to the melting of the

$$\underset{(3:1)}{\text{compound}} \rightarrow \text{liquid} \qquad (4)$$

and is also nonvariant with composition in accordance with the

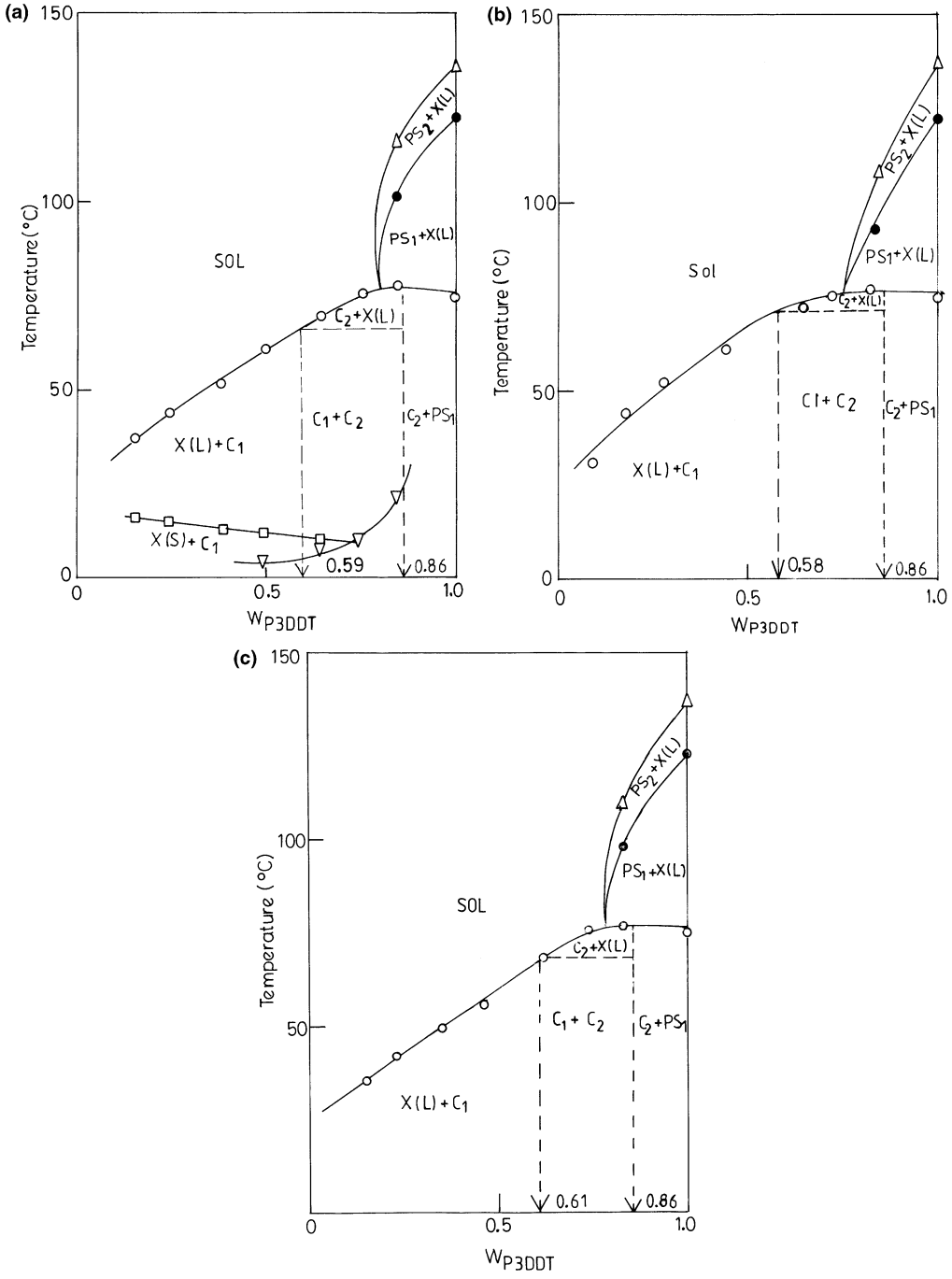

Figure 7. Phase diagram of (a) P3DDT−*p*-Xy gels, (b) P3DDT−*o*-Xy gel, and (c) P3DDT−*m*-Xy gel: (△,●) main chain melting; (○) side chain melting; (□, ▽) solvent melting. In the phase diagrams, the notations are X(L) = xylene liquid state, X(S) = xylene solid state, C_1 = 2:3 compound, C_2 = 3:1 compound, and PS_1 and PS_2 = polymer solid state-1 and polymer solid state 2. The plus sign indicates the simultaneous presence of two phases.

phase rule. In the figure, the indistinguishable nonvariant transition is shown by the dotted line as this is not directly detected in DSC thermograms. The phase diagrams of P3DDT−*o*-Xy and P3DDT−*m*-Xy systems are very much similar to each other and also similar to that of the polymer part of the P3DDT−*p*-Xy system (Figure 7b,c).

The phase behavior of *p*-Xy in the gel is also shown in the bottom part of Figure 7a. There is a decrease in melting temperature of the solvent with increase of W_{P3DDT}. At the intermediate compositions, it bifurcates, and the melting point of lower melting component increases with increase of W_{P3DDT}. Though we cannot afford any definite explanation, it might be due to the free solvent (intercalated) and bound solvent present in the gel; with increase of W_{P3DDT}, the melting point of bound solvent may increase. It is necessary to mention here how the two different polymer−solvent compounds are produced in this P3DDT−*p*-Xy system. At the stoichiometric composition of the 2:3 complex, not all of the *p*-Xy molecules are tightly bound with the polymer chain; some solvent molecules may remain intercalated within the two polymer−solvent layers. Upon increase of the P3DDT concentration or temperature, the intercalated solvent molecules may come out from the 2:3 complexes and complexes of 3:1 type are produced. So at certain regions of the phase diagram, there may exist both of the compounds, and this is evident in the phase diagrams at the composition range W_{P3DDT} = 0.59−0.86 (below 66 °C). At

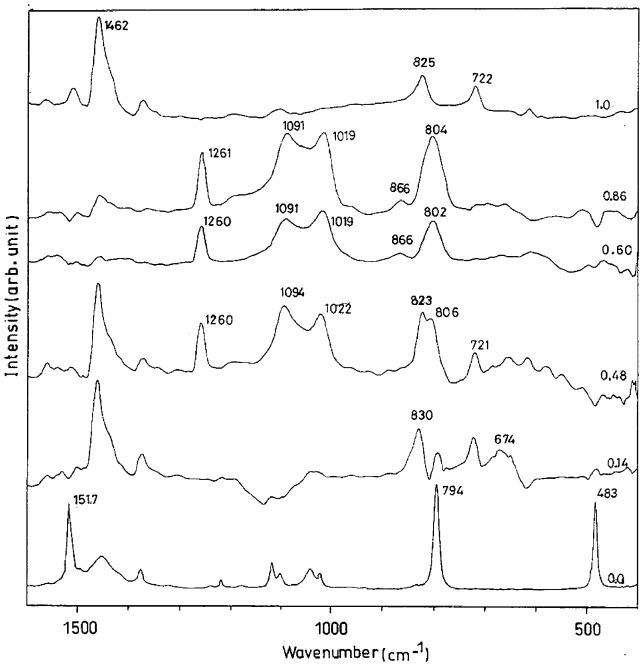

Figure 8. Solvent-subtracted FTIR spectra of P3DDT−*p*-Xy gels at indicated P3DDT weight fractions.

compositions $W_{P3DDT} < 0.59$, only the 2:3 compound (C_1) exists, and at compositions $W_{P3DDT} > 0.86$, only the 3:1 compound (C_2) exists up to a certain temperature range.

FTIR Investigation. To get a further idea of polymer−solvent complexation, FTIR study of the gels was done. The solvent-subtracted FTIR spectra of P3DDT gels at different P3DDT concentrations and the FTIR spectra of pure components are presented in Figure 8. A comparison of the FTIR spectra of pure solvent and the gels ($W_{P3DDT} = 0.86$, 0.60, 0.48) indicates that the solvent peaks at 1517 and 483 cm^{-1} are completely subtracted. Therefore, the peaks at 1260, 1091, 1019, 866, and 804 cm^{-1} are newly developed and may be attributed to the polymer−solvent complexation. However, in the gel with composition $W_{P3DDT} = 0.14$, the above peaks are absent and new peaks at 830 and 674 cm^{-1} are observed. This might be considered for polymer−solvent complexation with different structure from the gels of composition $W_{P3DDT} = 0.48-0.86$. So it may be surmised from the FTIR results that some new peaks are observed for polymer−solvent complexation. The polymer−solvent complexes of compositions 0.48, 0.60, and 0.86 have approximately the same structure; however, the polymer−solvent complex produced at $W_{P3DDT} = 0.14$ is different from those of other gel compositions studied here.

WAXS Investigation. To understand the structure of gels more clearly, we studied the WAXS patterns of the as prepared gels, and in Figure 9, a comparison of those of melt crystals and gels of different compositions is presented. It is apparent from the figure that there is a significant difference among them, particularly at lower diffraction angles. The interchain lamellar spacing of the melt-quenched P3DDT and the gel ($W_{P3DDT} = 0.86$) is the same (26.6 Å), but it shifts to higher value (52 Å) for the gel of composition $W_{P3DDT} = 0.59$. It is absent in the gel of composition $W_{P3DDT} = 0.14$. So it may be surmised from the results that with dilution the interchain lamellar distance becomes longer and for the gel with lower P3DDT concentration ($W_{P3DDT} \leq 0.14$) interchain lamellar structure is lost. In Table 2, the peak positions and intensity ratio (I^0_{hkl}/I^0_{411}) of X-ray diffraction peaks are presented. The I^0_{hkl}/I^0_{411} ratio is found to change in the gels compared with those in the melt crystals. A

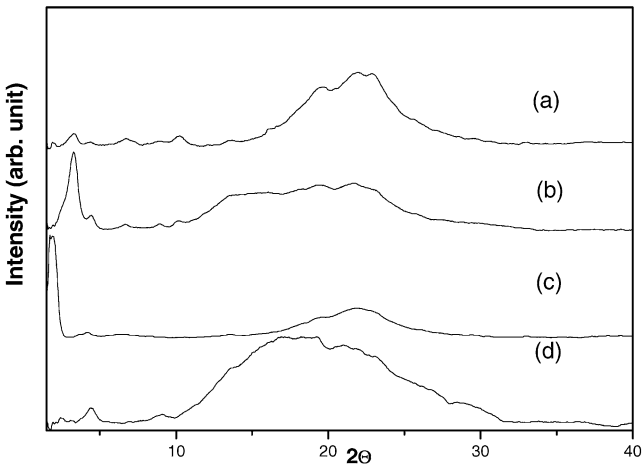

Figure 9. WAXS patterns of the as-prepared P3DDT−*p*-Xy gels: (a) $W_{P3DDT} = 1.0$; (b) $W_{P3DDT} = 0.86$; (c) $W_{P3DDT} = 0.59$; (d) $W_{P3DDT} = 0.14$.

TABLE 2: Peak Positions and the Intensity Ratio (I^0_{hkl}/I^0_{411}) of P3DDT Melt Crystals and P3DDT−*p*-Xy Gels at Different Weight Fractions of P3DDT

		I^0_{hkl}/I^0_{411}			
2θ (obsd)	hkl[14]	melt crystal	$W_{P3DDT} = 0.86$	$W_{P3DDT} = 0.59$	$W_{P3DDT} = 0.14$
4.36		0.05	0.35	0.17	0.21
6.70	200	0.10	0.17	0.10	0.03
8.83		0.06	0.18	0.04	0.13
10.21	300	0.13	0.24		
13.48	400	0.07		0.09	
16.63	011	0.27	0.82	0.18	1.16
18.30	401		0.89	0.48	1.15
	211				
19.66	311	0.80	0.97	0.69	1.16
20.98					1.04[a]
21.97	411	1.00	1.00	1.00	1.00
22.87	020	0.97		0.91	0.89
25.60	320	0.36		0.26	
29.83	810		0.20	0.07	0.29
	520				

[a] A new peak for polymer−solvent complexation.

probable explanation might be because polymer−solvent complexes produced in the systems induced a strain in the unit cell causing the I^0_{hkl}/I^0_{411} to change. In case of the gel of composition $W_{P3DDT} = 0.14$, a new peak at $2\theta = 20.98°$ is observed, and it might be due to polymer−solvent complexation. A probable explanation for the increase of interchain lamellar spacing for the above gels may be obtained from the molecular modeling given in the next section.

Molecular Modeling (MMX Program). To understand the formation of polymer−solvent complexes, molecular modeling using the MMX program has been done to get an approximate idea of the structure of the complexes. In Figure 10a,b, the molecular models of the P3DDT crystal and the 3:1 compound are presented. It is apparent from the figure that there is side chain crystallization with lamella distance of 28.7 Å (experimental value 26.6 Å). Thus, the lamellar structure of the P3DDT crystal may be approximately explained from side chain crystallization of the dodecyl groups.

Upon incorporation of some *p*-xylene molecules in the P3DDT crystal to make the composition approximately 3:1 (monomeric unit of P3DDT/*p*-xylene) the interchain lamellar distance increased by 0.3 Å. From the X-ray data, the interchain lamellar distance obtained is 0.2 Å greater than that of melt

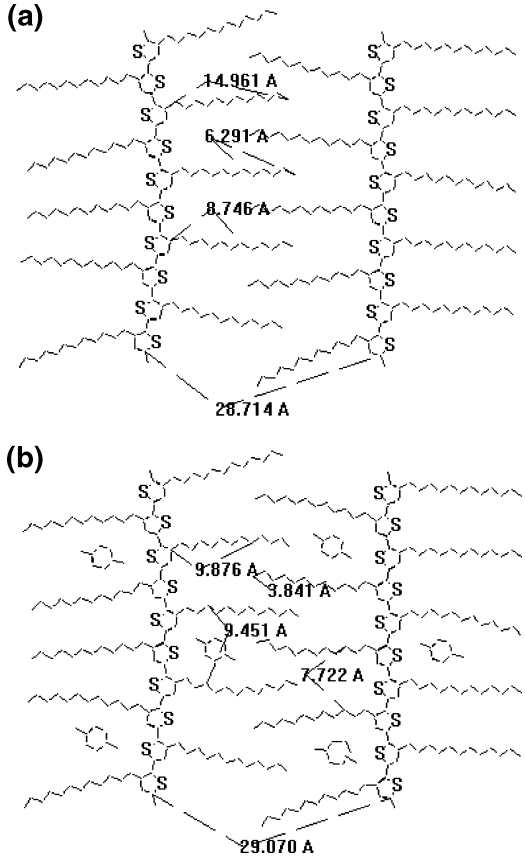

Figure 10. Molecular models of P3DDT−*p*-Xy gels using molecular mechanics (MMX) program: (a) pure P3DDT; (b) polymer−solvent complex of composition P3DDT/*p*-Xy = 3:1.

crystals. Further incorporation of *p*-xylene increases the interchain lamellar thickness, for example, an approximately 2:3 composition of the P3DDT−*p*-Xy system shows an interchain lamellar thickness of 36 Å. Experimentally in this system, we obtained the interchain lamellar thickness value of 52 Å. These results indicate that upon inclusion of solvent molecules between the interchain lamella the lamellar distance gradually increases and in very dilute solution the lamellar structure breaks. Probably each P3DDT chain becomes rigid by formation of polymer−solvent complexes and yields a stable rodlike conformer that aggregates to produce the gel. This might be a reason for the difference in FTIR spectra of the $W_{P3DDT} = 0.14$ gel compared to those of higher concentrations.

Conclusion

From the thermodynamic study, it may be concluded that during gelation of P3DDT−*p*-xylene systems polymer−solvent complexes are produced. In P3DDT−*o*- or *m*-xylene systems, the compositions of the complexes are also same, namely, 2:3. Analysis of the solvent-melting peak of the P3DDT−*p*-Xy system indicates another polymer−solvent complex of composition 3:1. Solvent-subtracted FTIR spectra indicated new absorbance peaks for polymer−solvent complex formation, and WAXS study indicated that lamella thickness of P3DDT gradually increases with incorporation of solvent molecules in the lamella. In dilute gels ($W_{P3DDT} = 0.14$), lamellar structure is totally lost. Molecular modeling supports that the inclusion of solvent molecules increases the interchain lamellar thickness.

Acknowledgment. We gratefully acknowledge CSIR Grant No. 1 (1655)/00 EMR-II for financial support.

References and Notes

(1) McCullough, R. D.; Ewbank, P. C. In *Handbook of Conducting Polymers*, 2nd ed.; Skotheim, T. A., Elsenbaumer, R. L., Reynolds, J. R., Eds.; Marcel Dekker: New York, 1998; p 225.
(2) Kobashi, M.; Takeuchi, H. *Macromolecules* **1998**, *31*, 7273.
(3) Malik, S.; Jana, T.; Nandi, A. K. *Macromolecules* **2001**, *34*, 275.
(4) Malik S. Ph.D. Thesis, Jadavpur University, Kolkata, 2002.
(5) Daniel, C.; Dammer, C.; Guenet, J.-M. *Polym. Commun.* **1994**, *35*, 4243.
(6) Guenet, J.-M.; Mckenna, G. B. *Macromolecules* **1988**, *21*, 1752.
(7) Guenet, J.-M. *Thermochim. Acta* **1996**, *284*, 67.
(8) Dikshit, A. K.; Nandi, A. K. *Macromolecules* **2000**, *33*, 2616.
(9) Tan, H. M.; Hiltner, A.; Moet, A.; Baer, E. *Macromolecules* **1983**, *16*, 28.
(10) Daniel, C.; Deluca, M. D.; Guenet, J. M.; Brulet, A.; Menelle, A. *Polymer* **1996**, *37*, 1273.
(11) Spevacek, J.; Saini, A.; Guenet, J. M. *Macromol. Rapid Commun.* **1996**, *17*, 389.
(12) Sakai, M.; Sotoh, N.; Tsujil, K.; Zhang, Y. Q.; Tanaka, T. *Langmuir* **1995**, *11*, 2493.
(13) Park, K. C.; Levon, K. *Macromolecules* **1997**, *30*, 3175.
(14) Tashiro, K.; Ono, K.; Minagawa, Y.; Kobayashi, M.; Kawai, T.; Yoshino, K. *J. Polym. Sci., Polym. Phys.* **1991**, *29*, 1223.
(15) Tipton D. L.; Russo, P. S. *Macromolecules* **1996**, *29*, 7402.
(16) Schmidtke, S.; Russo, P.; Nakamatsu, J.; Buyuktanir, E.; Turfan, B.; Temyanko, E. *Macromolecules* **2000**, *33*, 4427.
(17) (a) Mal, S.; Nandi, A. K. *Langmuir* **1998**, *14*, 2238. (b) Malik, S.; Maji, S. K.; Banerjee, A.; Nandi, A. K. *J. Chem. Soc., Perkin Trans. 2* **2002**, 1177.
(18) Liu, Y.; Pandey, R. B. *J. Chem. Phys.* **1996**, *105*, 825.
(19) Takahashi, M.; Shimazaki, M.; Yamamoto, J. *J. Polym. Sci., Part B* **2001**, *39*, 91.
(20) Domszy, R. C.; Alamo, R.; Edwards, C. O.; Mandelkern, L. *Macromolecules* **1986**, *19*, 310.
(21) Rughoopath, S. D. D. V.; Hotta, S.; Heeger, A. J.; Wudl, F. *J. Polym. Sci., Polym. Phys. Ed.* **1987**, *25*, 1071.
(22) Russo, P. S.; Miller, W. G. *Macromolecules* **1983**, *16*, 1690.
(23) Flory, P. J. *Proc. R. Soc. London, Ser. A* **1956**, *234*, 60.
(24) Malik, S.; Nandi A. K. *J. Polym. Sci., Polym. Phys.* **2002**, *40*, 2073.
(25) Liu, S. L.; Chung, T. S. *Polymer* **2000**, *41*, 2781.
(26) Nijenhuis, K. te. *Adv. Polym. Sci.* **1997**, *130*, 1.
(27) Chen, T.-A.; Wu, X.; Rieke, R. D. *J. Am. Chem. Soc.* **1995**, *117*, 233.
(28) Amou, S.; Hota, O.; Shiroto, K.; Hayakawa, J.; Ueda, M.; Takeuchi, K.; Asai, M. *J. Polym. Sci., Polym. Chem.* **1999**, *37*, 1943.
(29) Gajewski, K. E.; Gillberr, M. H. In *Advances in Molecular Modeling*; Liotta, D., Ed.; Jai Press: Greenerick, CT, 1990; Vol. 2.
(30) Saini, A.; Spevacek, J.; Guenet, J. M. *Macromolecules* **1998**, *31*, 703.
(31) Reisman, A. *Phase Equilibria*; Academic Press: New York, 1970.